

Coefficient of Earth Pressure at Rest

Figure 12.20 on Page 561

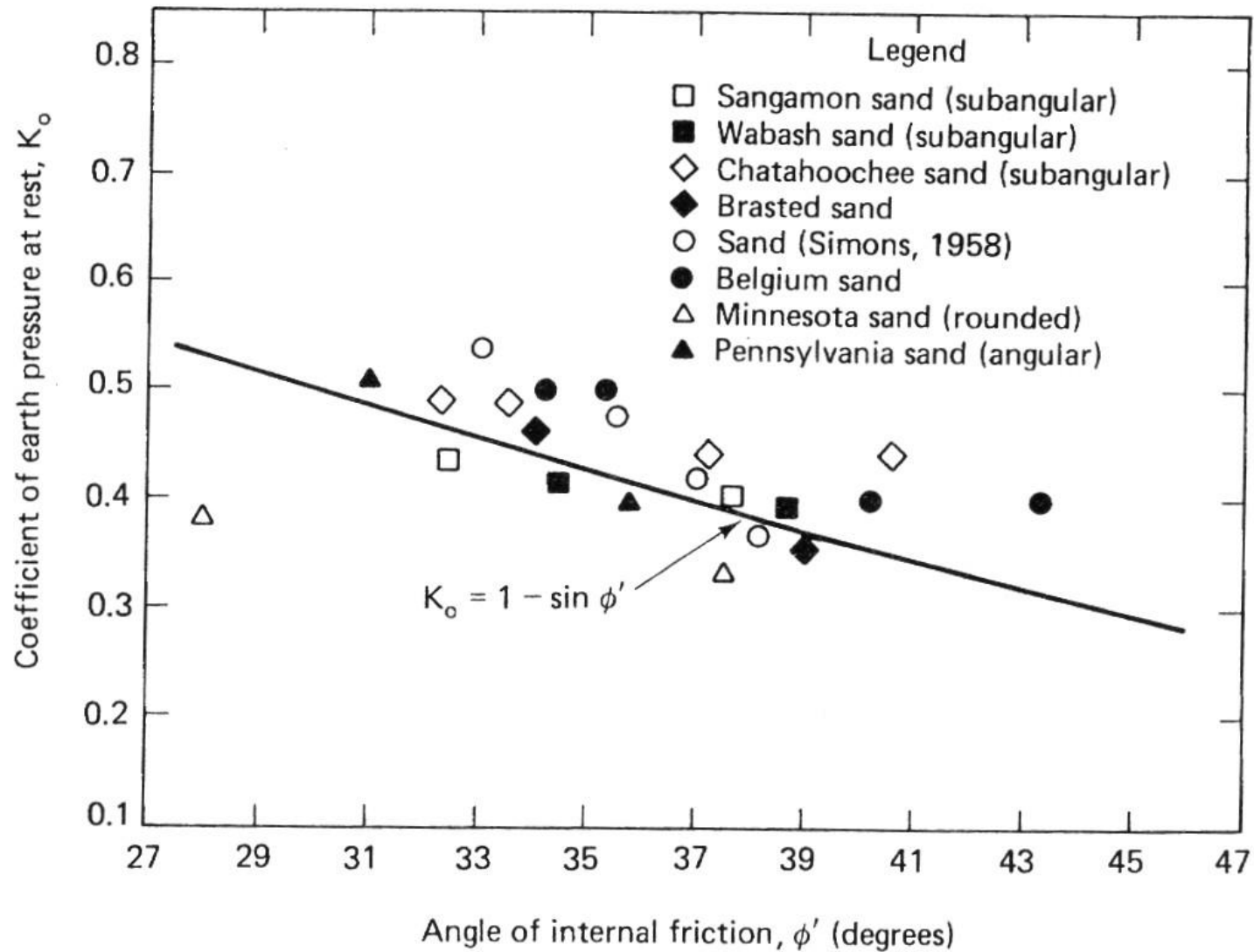


Fig. 11.14 Relationship between K_o and ϕ' for normally consolidated sands (after Al-Hussaini and Townsend, 1975).

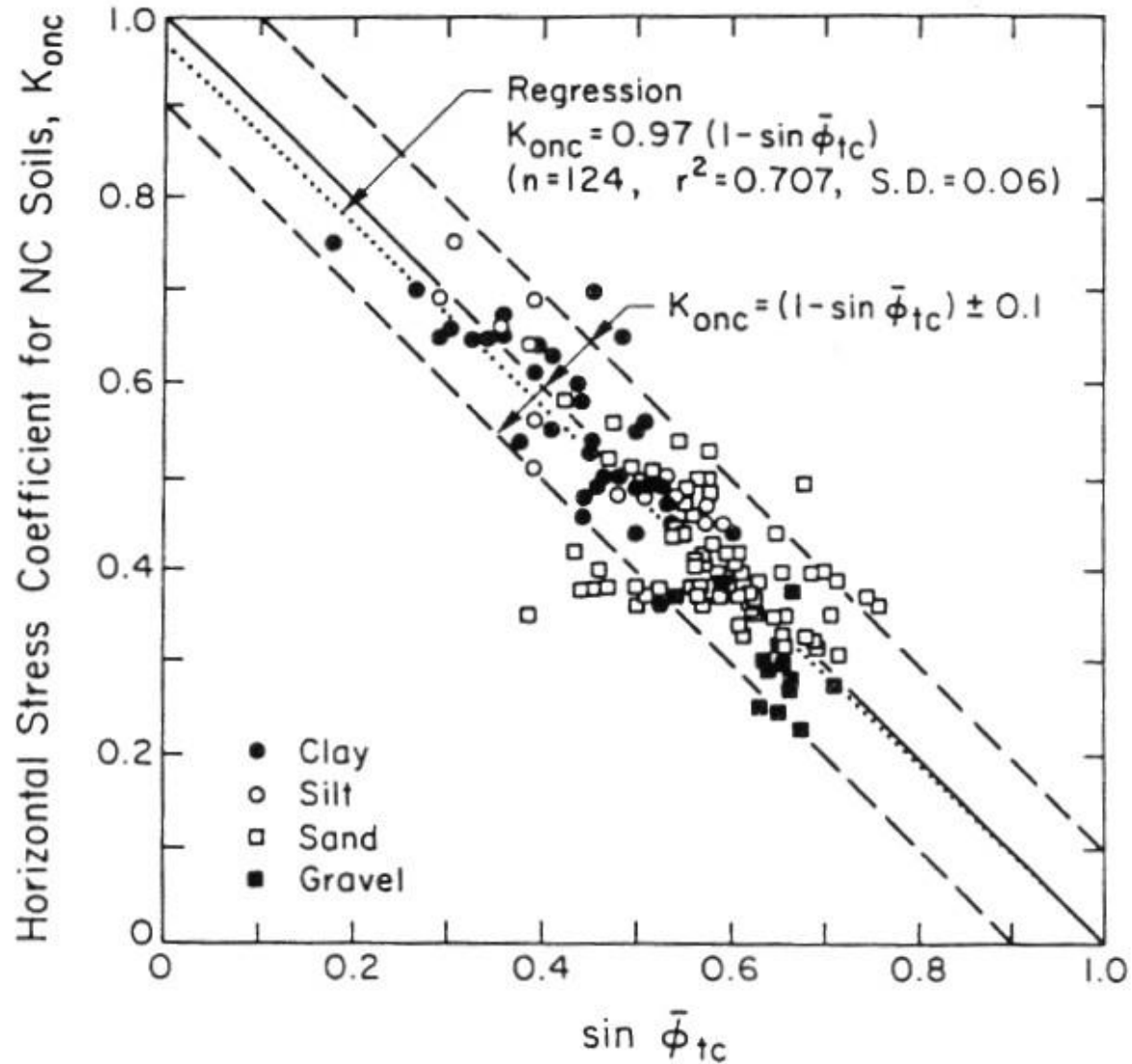


Figure 3-3. Horizontal Stress Coefficient for NC Soils from Laboratory Tests

(Mayne & Kulhawy, *Manual on Estimating Soil Properties for Foundation Design*, 1990)

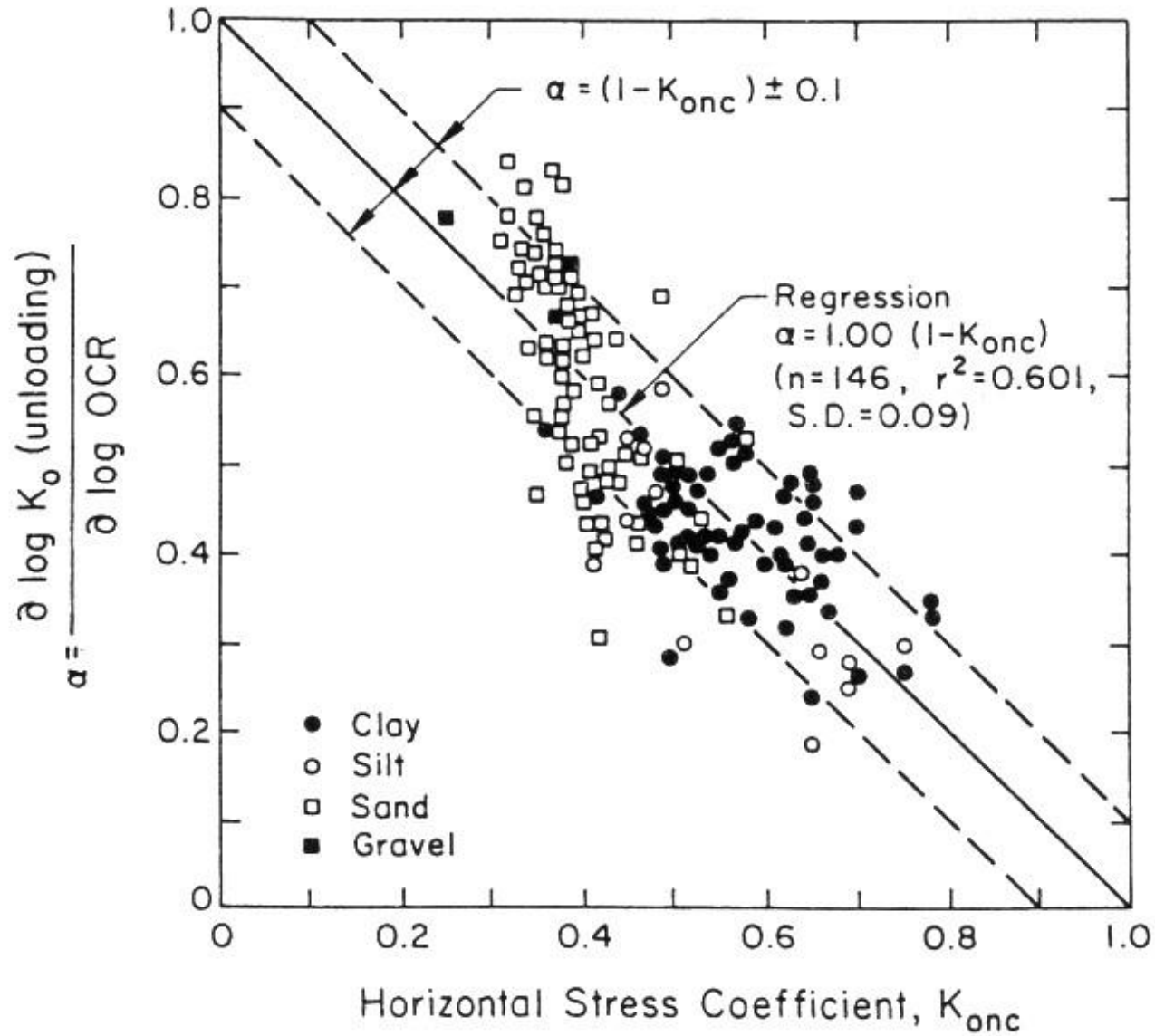


Figure 3-4. Unload Coefficient for OC Soils

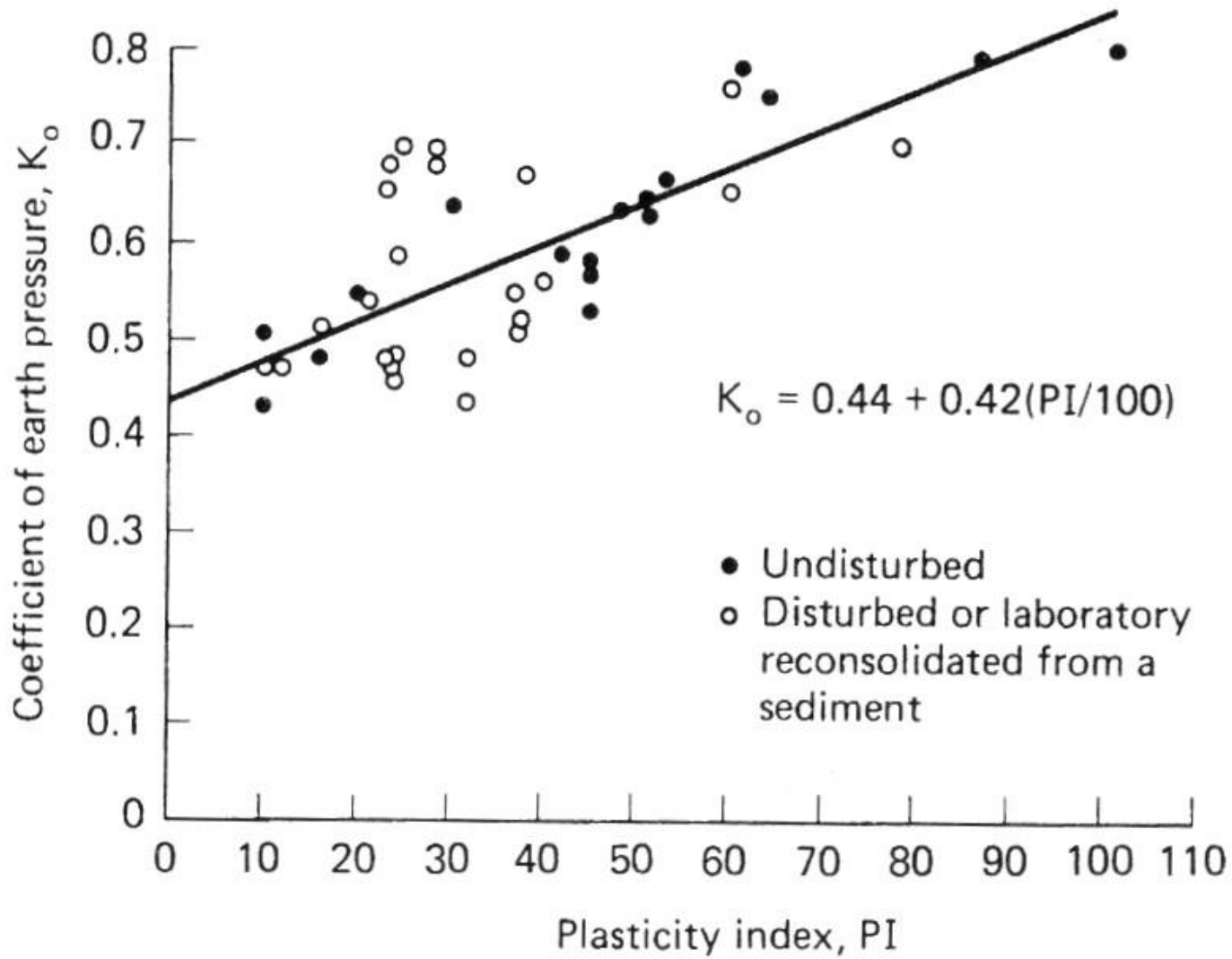


Fig. 11.69 Correlation between K_o from laboratory tests and plasticity index PI (after Massarsch, 1979).

Figure 12.55 on Page 595

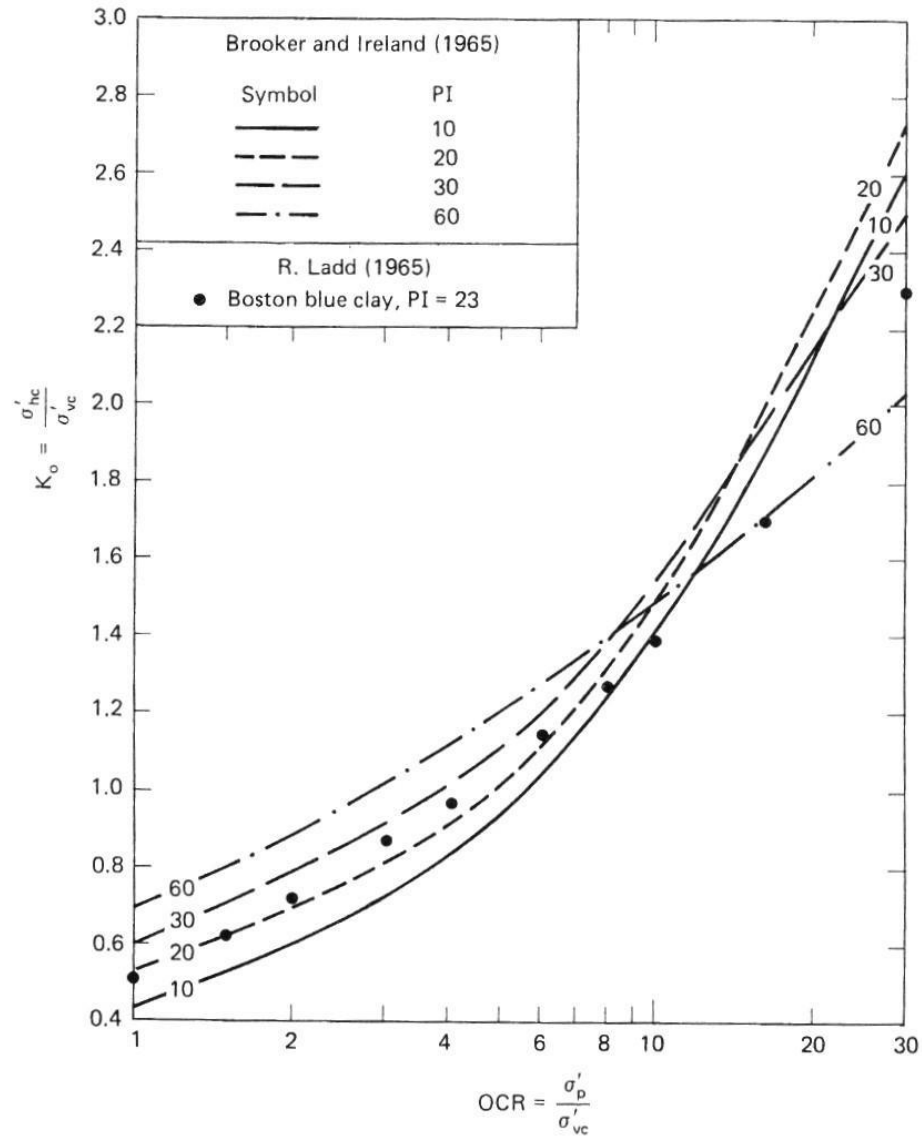


Fig. 11.72 K_0 versus OCR for soils of different plasticities. The data by Brooker and Ireland (1965, Fig. 11) was replotted by Ladd (1971a).

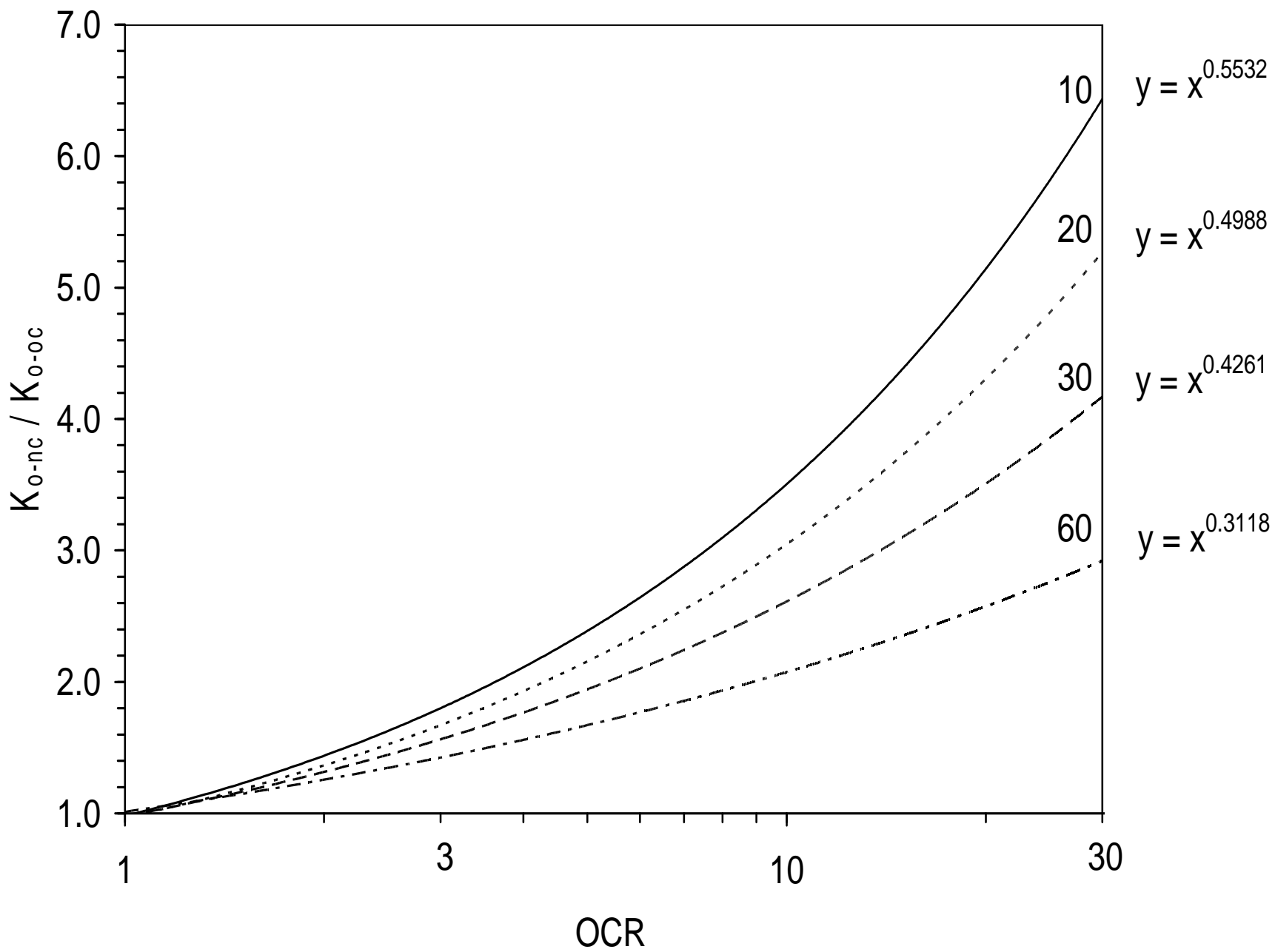
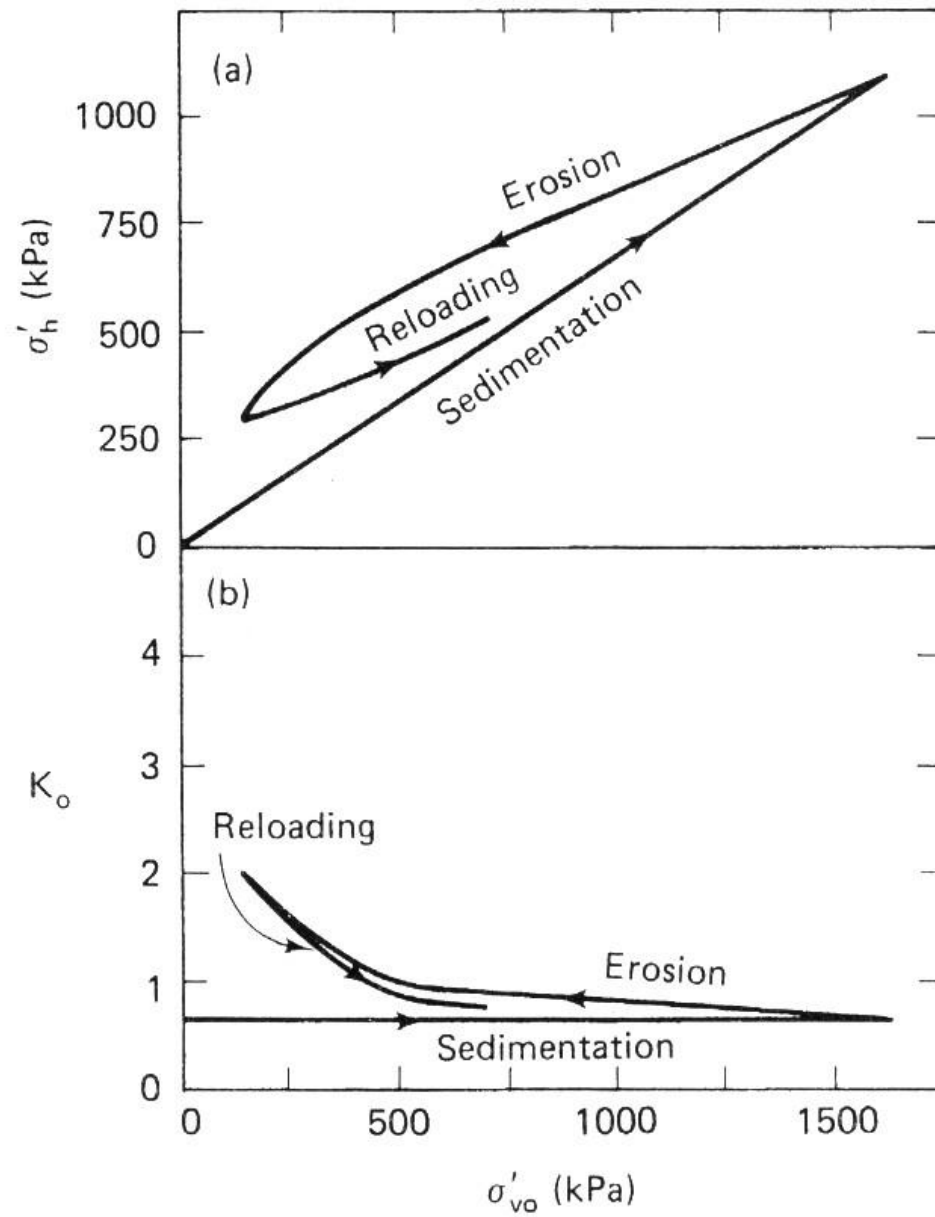


Figure 12.51 on Page 594



Stress Paths During Undrained Loading

Figure 13.16 on Page 630

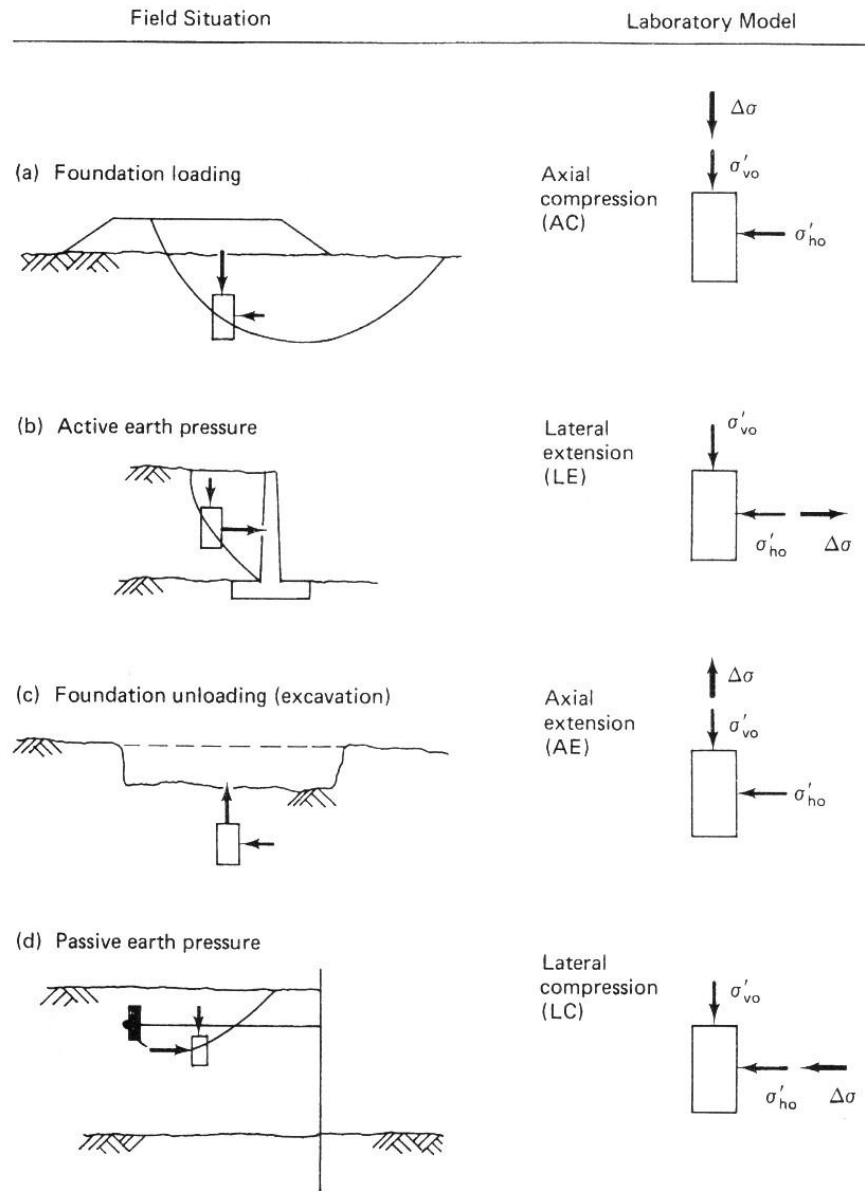


Fig. 11.73 Some common field stability situations along with their laboratory model.

Figure Ex. 13.6c on Page 637

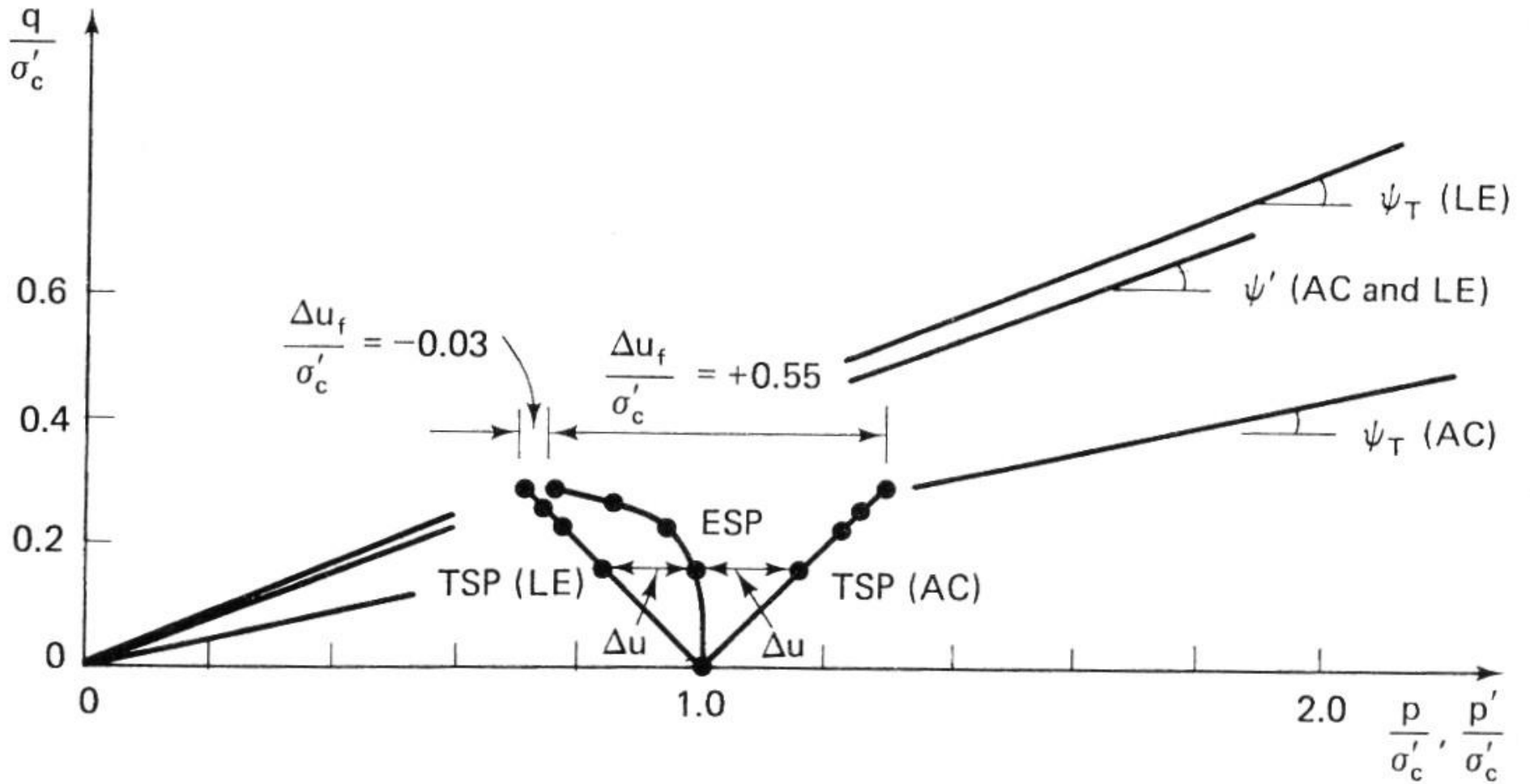


Fig. Ex. 11.17c Stress paths for the AC and LE tests.

Figure Ex. 13.6d on Page 639

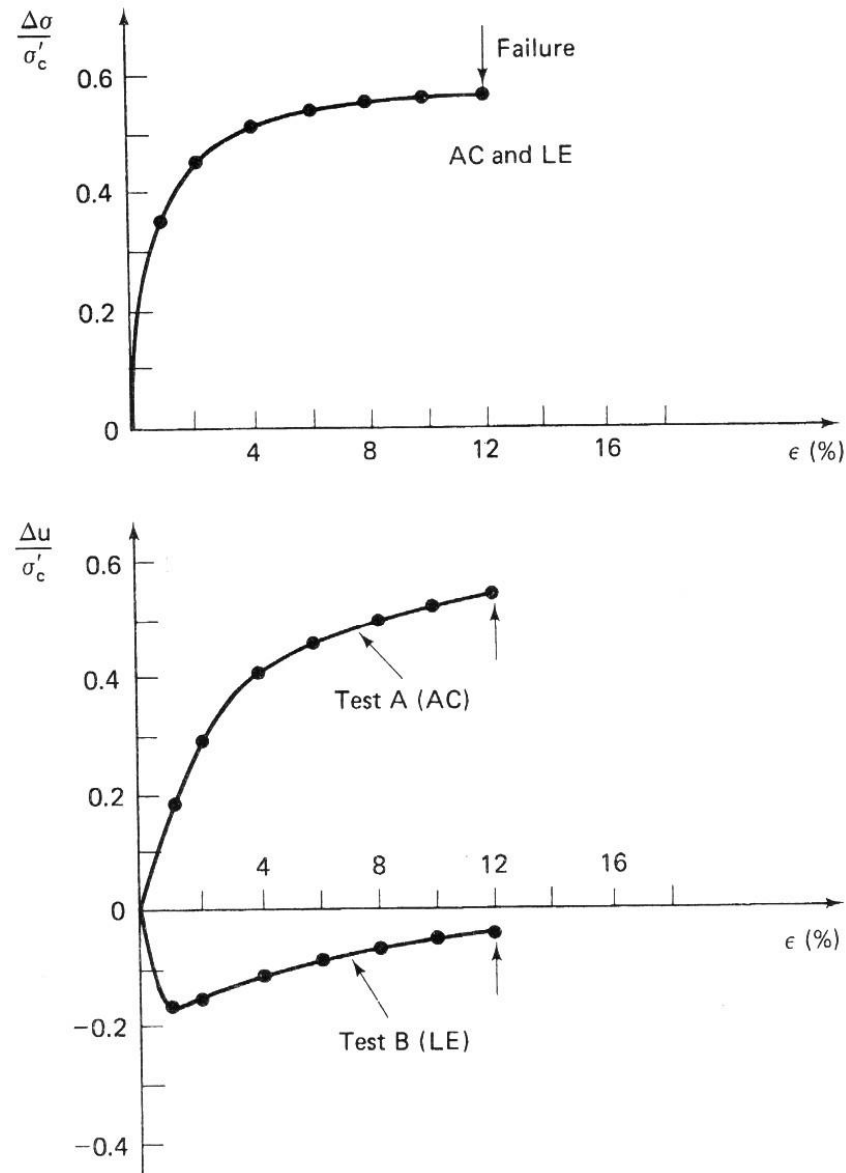


Fig. Ex. 11.17d Stress-strain and pore pressure-strain data for both tests.

Figure 13.19 on Page 641

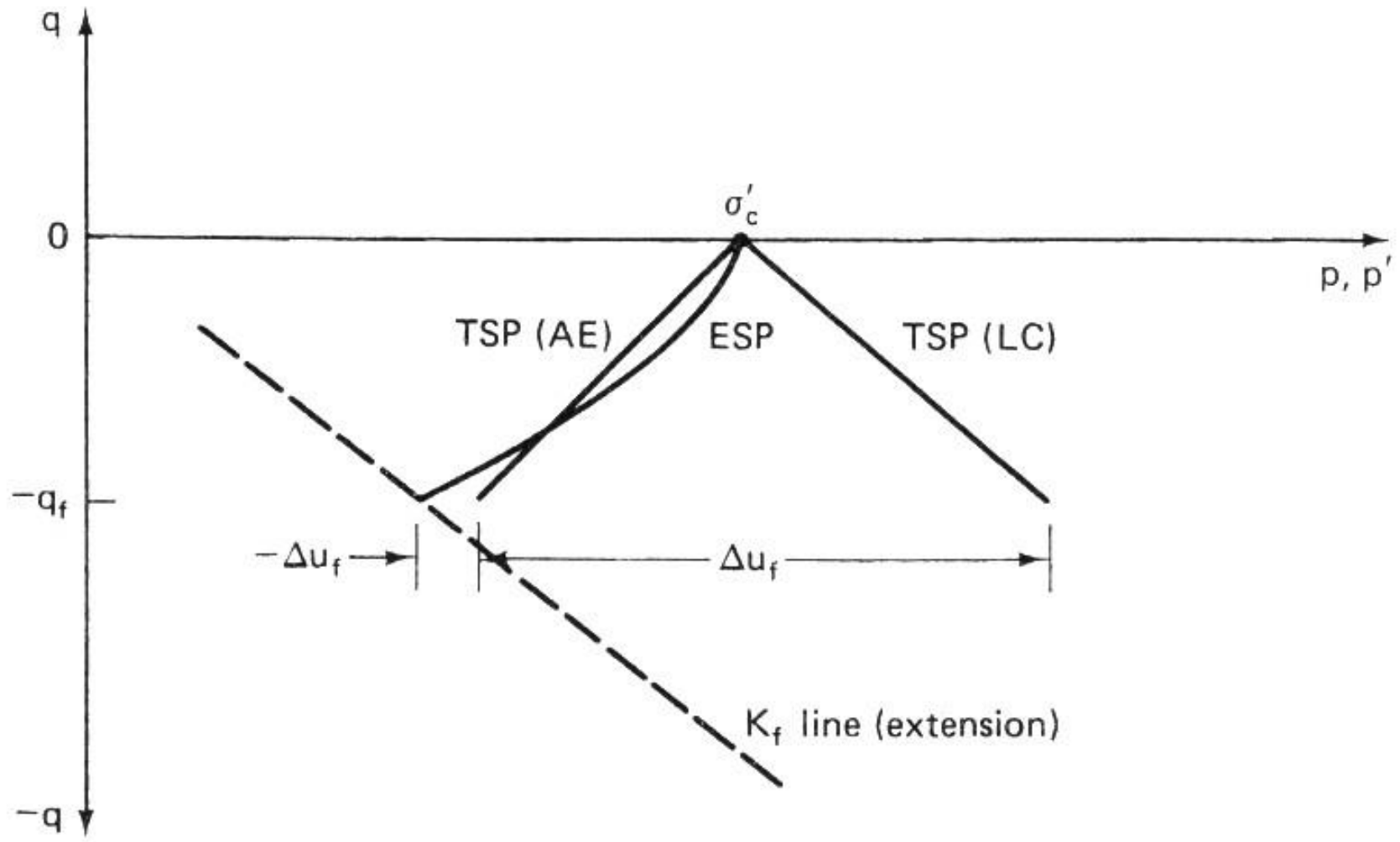


Fig. 11.76 Stress paths for the AE and LC tests—normally consolidated clay.

(Holtz & Kovacs, *An Introduction to Geotechnical Engineering*, 1981)

Figure 13.18 on Page 641

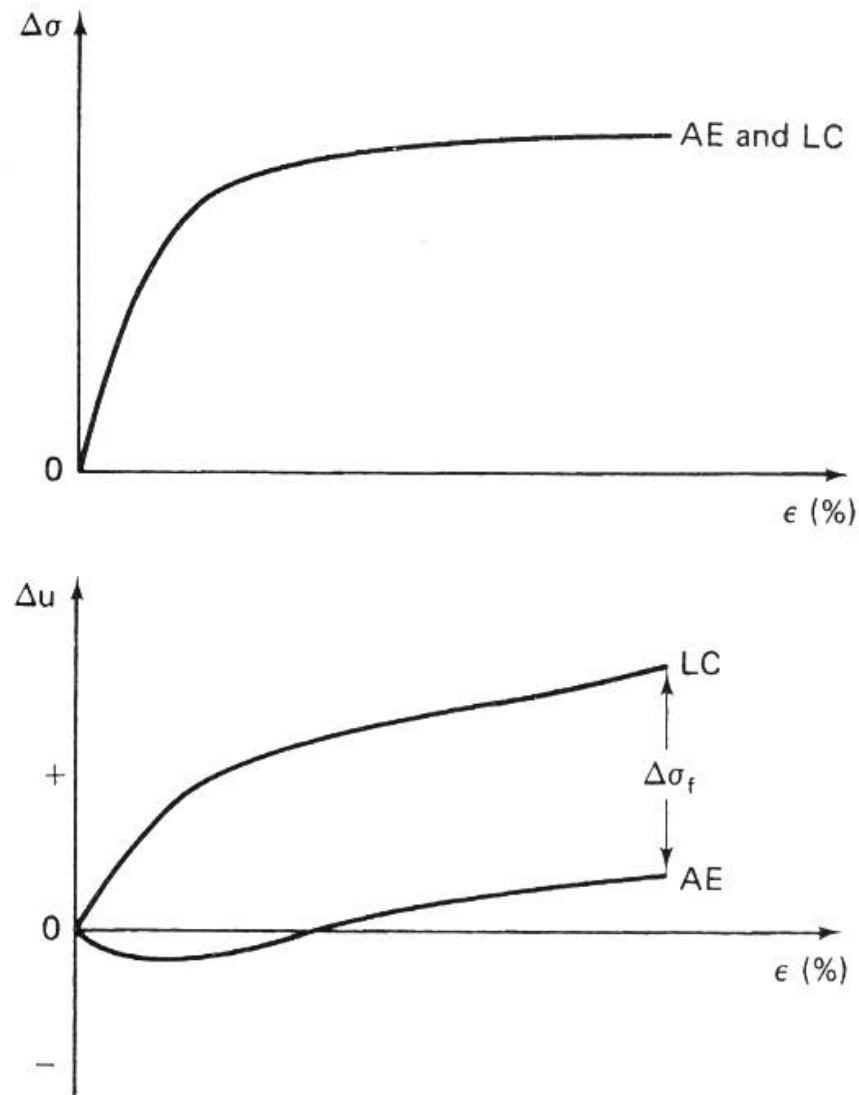


Fig. 11.75 Stress-strain and pore pressure-strain curves for AE and LC tests on a normally consolidated clay (after Hirschfeld, 1963).

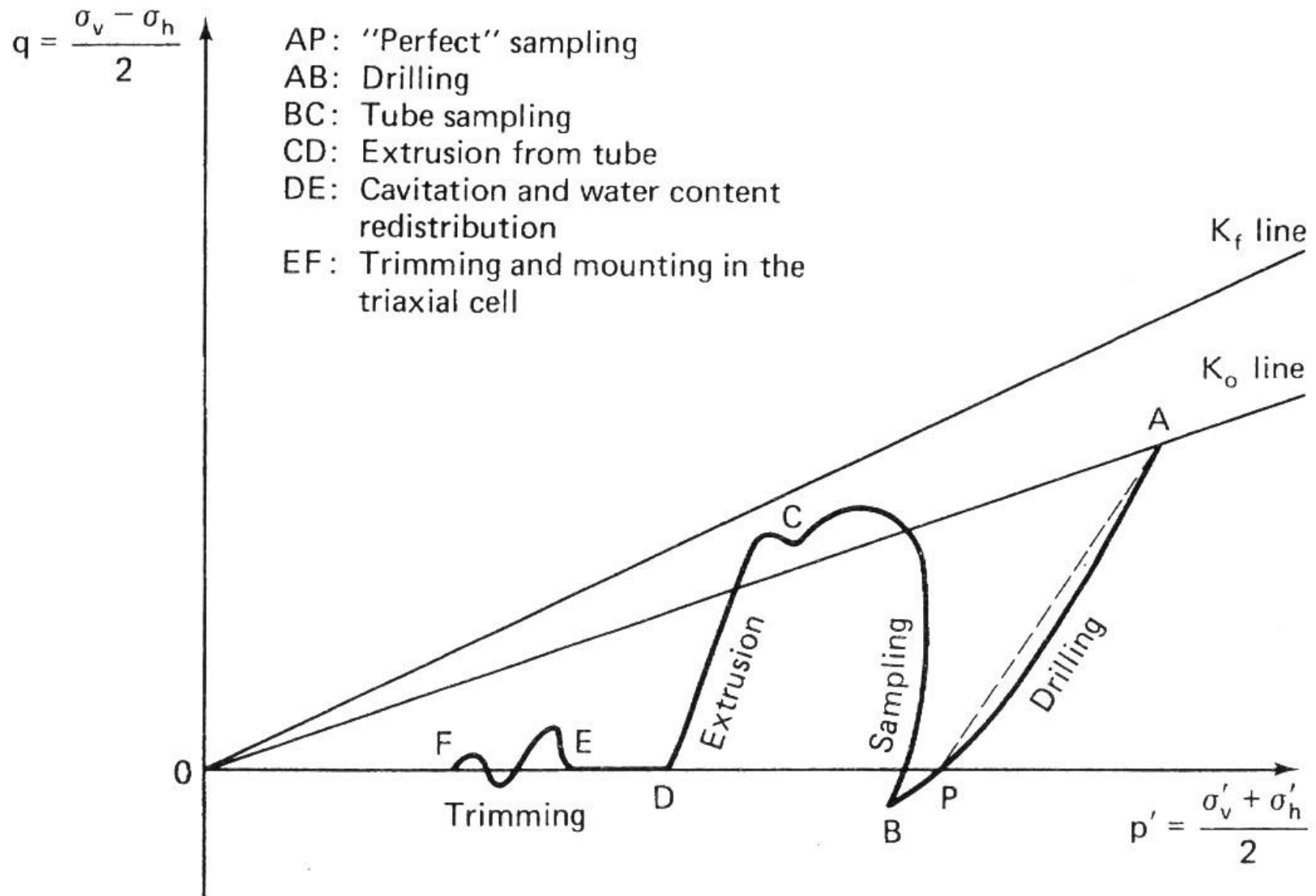


Fig. 11.81 Stress paths during sampling of a normally consolidated clay (after Ladd and Lambe, 1963).

Figure 13.25a on Page 649

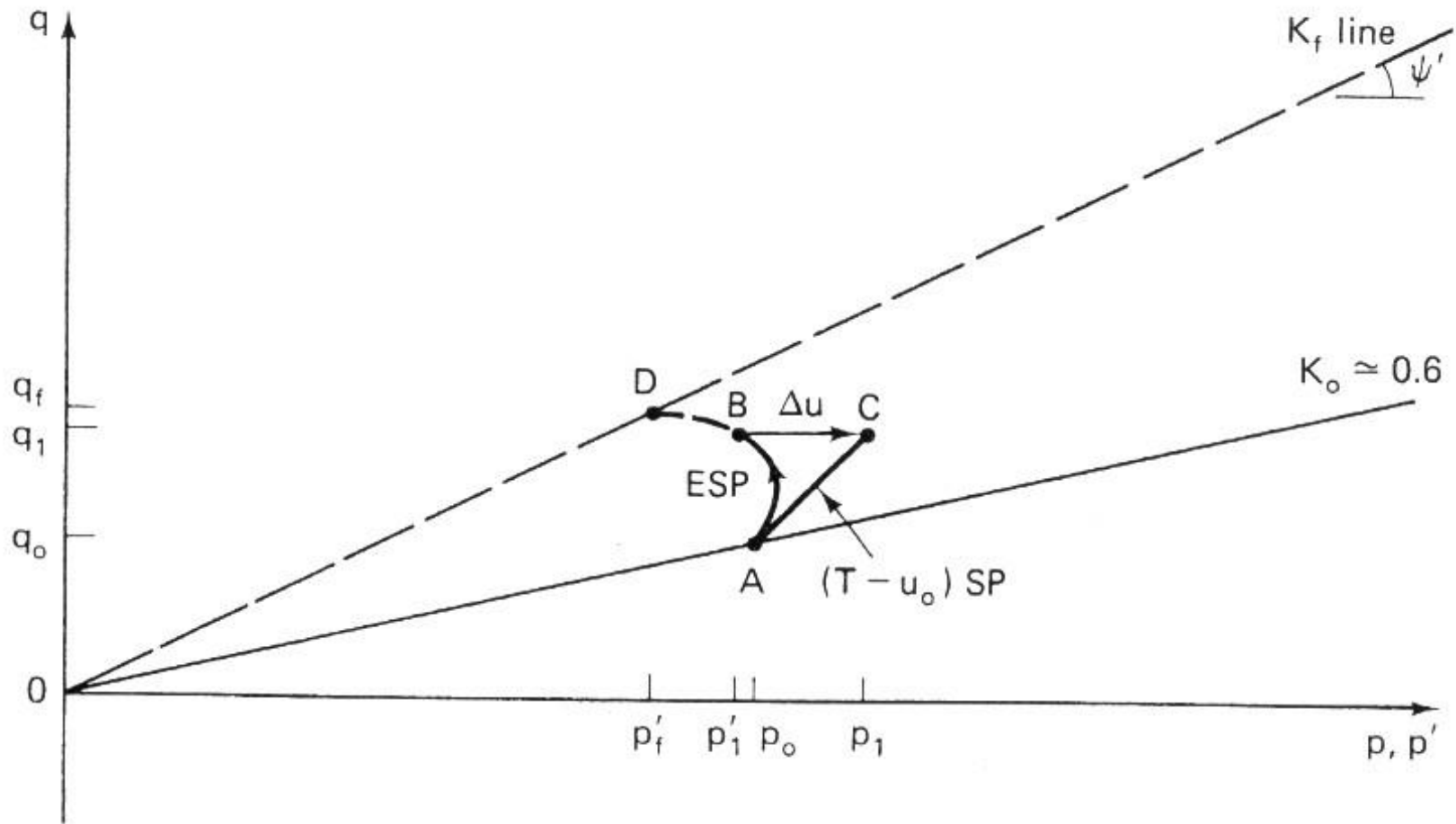


Figure 13.13b on Page 625

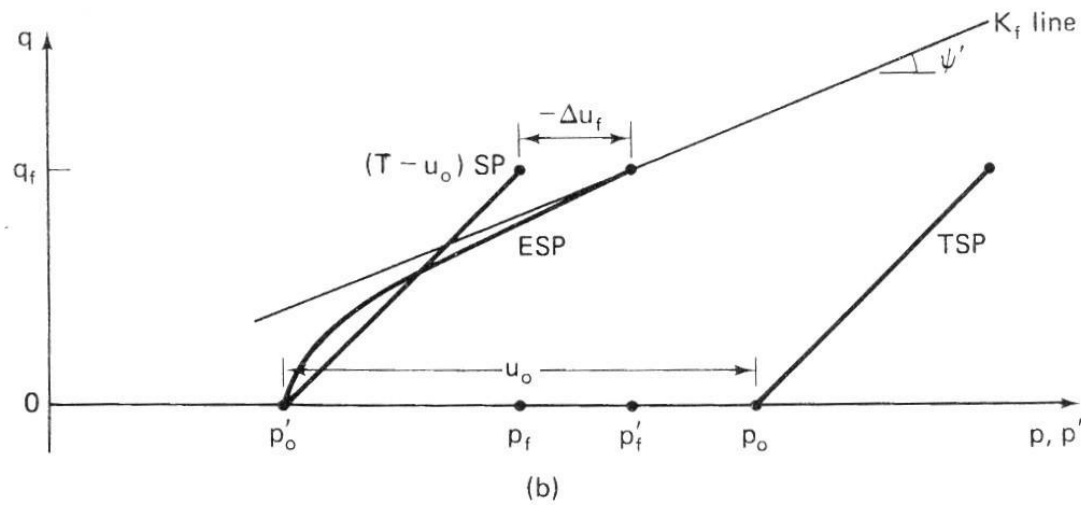
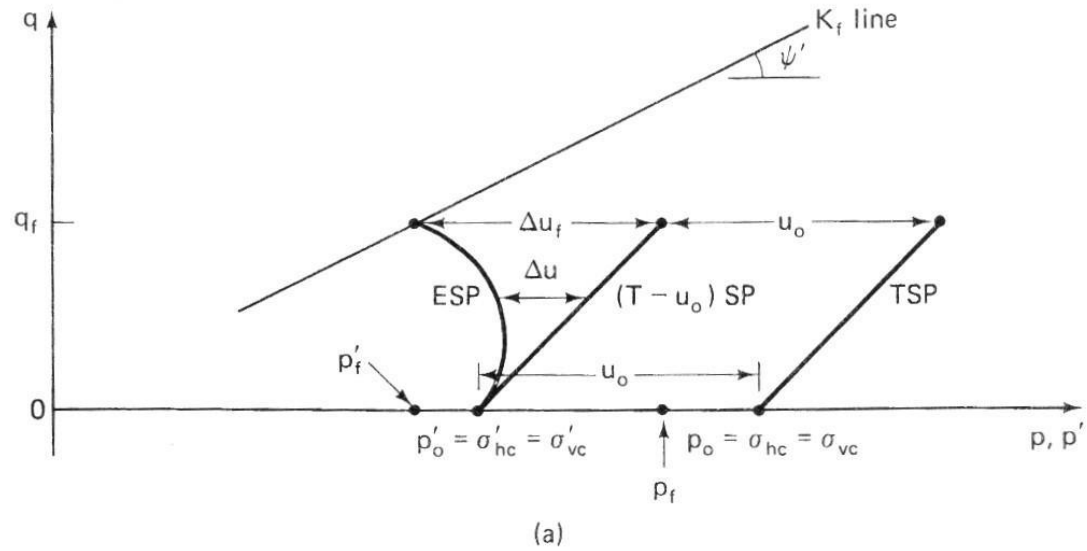


Fig. 11.34 Stress paths for the hydrostatically consolidated axial compression tests on (a) normally consolidated clays; (b) overconsolidated clays.

Figure 13.25b on Page 649

